Donepezil, an acetylcholinesterase inhibitor against Alzheimer's dementia, promotes angiogenesis in an ischemic hindlimb model

Yoshihiko Kakinuma, Mutsuo Furihata[1], Tsuyoshi Akiyama[2], Mikihiko Arikawa, Takemi Handa, Rajesh G. Katare, Takayuki Sato

Department of Cardiovascular Control, [1]Department of Pathology, Kochi Medical School, Nankoku, Japan
[2]Department of Cardiac Physiology, National Cardiovascular Center Research Institute, Suita, Japan

Running title: Donepezil regulates angiogenesis.

Corresponding author:

Yoshihiko Kakinuma, MD, PhD
Department of Cardiovascular Control
Kochi Medical School,
Nankoku, Kochi 783-8505
Japan

TEL: +81-(0)88-880-2587
FAX: +81-(0)88-880-2310
E-mail: kakinuma@kochi-u.ac.jp

Abstract

Introduction: Our recent studies have indicated that acetylcholine (ACh) protects cardiomyocytes from prolonged hypoxia through activation of the PI3K/Akt/HIF-1α/VEGF pathway, and that cardiomyocyte-derived VEGF promotes angiogenesis in a paracrine fashion. These results suggest that a cholinergic system plays a role in modulating angiogenesis. Therefore, we assessed the hypothesis that the cholinergic modulator donepezil, an acetylcholinesterase inhibitor utilized in Alzheimer's disease, exhibits beneficial effects, especially on the acceleration of angiogenesis.

Methods: We evaluated the effects of donepezil on angiogenic properties *in vitro* and *in vivo*, using an ischemic hindlimb model of α7 nicotinic receptor-deleted mice (α7 KO) and wild type mice (WT).

Results: Donepezil activated angiogenic signals, i.e., HIF-1α and VEGF expression, and accelerated tube formation in human umbilical vein endothelial cells (HUVECs). ACh and nicotine upregulated signal transduction with acceleration of tube formation, suggesting that donepezil promotes a common angiogenesis pathway. Moreover, donepezil-treated WT exhibited rich capillaries with enhanced VEGF and PCNA endothelial expression, recovery from impaired tissue perfusion, prevention of ischemia-induced muscular atrophy with sustained surface skin temperature in the limb, and inhibition of apoptosis independent of the α7 receptor. Donepezil exerted comparably more effects in α7 KO in terms of angiogenesis, tissue perfusion, biochemical markers, and surface skin temperature. Donepezil concomitantly elevated VEGF expression in intracardiac endothelial cells of WT and α7 KO, and further increased choline acetyltransferase (ChAT) protein expression, which is critical for ACh synthesis in endothelial cells.

Conclusion: The present study concludes that donepezil can act as a therapeutic tool to accelerate angiogenesis in cardiovascular disease patients.

Keywords: angiogenesis, vascular endothelial growth factor, acetylcholinesterase inhibitor, donepezil

Introduction

Studies investigating the effects of vagal nerve stimulation (VS) on heart failure have suggested VS as a candidate for a therapeutic modality in heart failure because VS suppresses infarction-induced fatal arrhythmia and progression of ventricular remodeling [1,2]. However, the precise mechanisms remain to be fully elucidated.

To further investigate the underlying mechanisms of the VS effects, we have focused on disclosing the pleiotrophic effects of acetylcholine (ACh) and revealed that ACh prevents cardiomyocytes from persistent hypoxia-induced cell death, and have ultimately presented a new concept regarding ACh as a trophic factor. Our recent study demonstrated that ACh directly transduces cell survival signal through the muscarinic receptor, activates the PI3K/Akt/HIF-1α/VEGF pathway, inhibits collapse of mitochondrial membrane potential, and inactivates caspase-3 in cardiomyocytes subjected to hypoxia [3]. Because both survival and angiogenic pathways share common signaling molecules through HIF-1α/VEGF, these results prompted us to speculate the involvement of ACh in modulation of angiogenesis.

Furthermore, ACh transduces signals through nitric oxide (NO) production, and NO plays a key role in angiogenesis [4-8]. Specifically, according to our previous study, the NO donor *S*-nitroso-*N*-acetylpenicillamine activates the PI3K/Akt/HIF-1α pathway to increase VEGF expression in cardiomyocytes, and VEGF derived from cardiomyocytes accelerates tube formation in human umbilical endothelial cells (HUVECs), i.e., *in vitro* angiogenesis [4].

In contrast to these positive results, few *in vivo* studies have demonstrated the effects of systemically administered ACh because of its severe side effects including induction of bronchospasm and airway mucus hypersecretion. To circumvent this, we used donepezil, an acetylcholinesterase inhibitor and anti-Alzheimer's drug, that elevates local levels of ACh without such adverse effects [9,10]. In addition, we tested the effect of donepezil in a murine hindlimb ischemia model. To extensively investigate the effect of donepezil, we used α7 nicotinic receptor-deleted mice (α7 KO) suffering from impaired angiogenesis with characteristic mechanisms [11-13]. In the present study, we demonstrated a novel effect of donepezil on angiogenesis, i.e., acceleration of angiogenesis.

Materials and Methods

Murine hindlimb ischemia model and donepezil administration

Male C57BL6/J mice (WT) (n = 45) and α7 KO (n = 26) aged 10 - 12 weeks were used. After anesthesia with pentobarbital sodium (30 mg/kg), the left femoral artery was completely ligated at its proximal end. Ligation was verified to be successful by pallor of the left foot. Donepezil (5 mg/kg/day) dissolved in drinking water (50 mg/L) was orally administered *ad lib* for 4 weeks. This dose was initially determined to clearly show the expected effects without producing adverse effects in the mice.

To investigate the involvement of cholinergic receptors on the effects of donepezil in terms of angiogenesis *in vivo* and to compare it with WT treated with donepezil alone, further donepezil-treated WT were divided into 3 subgroups (n = 6 - 9 in each group) receiving one of the following treatments for 4 weeks: (a) α-bungarotoxin (14 μg/kg/day by i.m. on the flank), (b) mecamylamine (2.1 mg/kg/day i.m. on the flank), and (c) atropine (5 mg/kg/day p.o.) [14]. Another experimental study was conducted on α7 KO with a lower dose (0.083 mg/kg/day) using the same experimental schedule (n = 9). This lower dose was comparable with that prescribed for patients. At the end of the treatment period, the heart and quadriceps femoris muscle were excised for experiments. Our preliminary study verified that even higher dose of donepezil, 5 mg/kg/day, does not downregulate heart rate or blood pressure.

Angiography using indocyanine green dye

To functionally evaluate the effects of donepezil on murine angiogenesis, angiography was performed using indocyanine green (ICG) (Sigma-Aldrich, St. Louis, MO, USA), which clearly visualize tissue perfusion in the hindlimb. After anesthesia with pentobarbital sodium, both lower extremities were shaved. The field was illuminated by a LED-fluorescence imaging device, and ICG was administered intravenously (0.3 mg/kg). After a bolus ICG injection, real-time imaging analysis was performed using an infrared camera, and recorded with a digital camcorder for an optimized time. Our preliminary studies identified that ICG angiography in the hindlimbs initially revealed an angiogram, followed by a perfusion phase, when the fluorescence signals in the perfused tissue were simultaneously and homogeneously increased in both hindlimbs. After recording, the fluorescence intensity in the hindlimb was evaluated. Therefore, to evaluate perfusion in an ischemic hindlimb, the interested regions were selected from both right and left hindlimbs. The fluorescence signals of the left hindlimb in the perfusion phase were compared with those of the right, using NIH image software, and it revealed laterality in

the ICG signal intensity. The time when the signal difference between the right and left was extremely evident was selected.

Evaluation of the relative blood flow using fluorescent microspheres

According to previous studies using fluorescent microspheres [15,16], we evaluated the relative blood flow between the left and right hindlimbs in mice. Briefly, after anesthesia, 200 μL of green FluoSphere fluorescent microspheres (15 μm, Molecular Probes, Invitrogen, Carlsbad, CA, USA) were administered within 1 min, followed by immediate sampling of blood and bilateral quadriceps femoris muscles. These samples were weighed accurately and incubated in 4 M KOH containing 2% of Tween 80 at 70ºC for 24 h. After measuring the fluorescence, the ratio of the fluorescence between the left and right hindlimbs, corrected by the tissue weight, was compared.

Thermography

One day after surgery, an initial temperature evaluation was performed in the hindlimbs using infrared thermography (MobIR M4 Thermal Camera, Wuhan Guide Infrared Technology Co., Ltd. China). The skin temperature of the mice under anesthesia was measured 3 times. Thereafter, for each mouse, temperature was evaluated 3 times by thermography during 4 weeks. The temperature distribution in the hindlimbs was compared between donepezil-treated and untreated mice, and standardized by each non-ligated hindlimb as a reference. The laterality in temperature, represented by the ratio between the left and right hindlimb temperature, was evaluated.

Immunohistochemistry

The heart and quadriceps femoris muscle were excised and fixed in 4% paraformaldehyde. Some muscle samples were routinely processed, paraffin-embedded, cut into 4 μm sections, and stained with hematoxylin and eosin. The number of nuclei in capillary-like structures per HPF were counted in randomly selected fields (9 fields per section). Other samples were used for immunohistochemical study using the Ventana automated immunohistochemistry system (Discovery TM, Ventana Medical System, Inc., Tucson, AZ, USA). Antigen retrieval was performed for 60 min in a preheated Dako Target Retrieval Solution (pH 6.0) using a microwave, followed by inhibition of intrinsic peroxidase, blocking, and the reaction with a primary antibody. VEGF and PCNA immunoreactivities were identified using a polyclonal anti-VEGF antibody at 1:100 (sc-152) (Santa Cruz Biotechnology, CA, USA) and a monoclonal anti-PCNA antibody at 1:2000 (Abcam Inc., Cambridge, MA, USA), respectively, based on the

streptavidin-biotin-peroxidase reaction.

Western blotting

Whole muscle cell lysates were fractionated by SDS–PAGE and transferred onto membranes (Millipore Corp., Bedford, MA, USA). The membranes were incubated with polyclonal antibodies against VEGF (Santa Cruz Biotechnology), ChAT (Millipore Corp., Bedford, MA, USA), cleaved caspase-3 (Cell Signaling Technology, Danvers, MA, USA), diluted at 1:500, or with monoclonal antibodies against HIF-1α (Novus Biologicals, Inc., Littleton, CO, USA), pFlk-1 (Tyr 951, Santa Cruz Biochemistry), diluted at 1:500, α-tubulin (LAB VISION, Fremont, CA, USA) and PCNA (Abcam Inc.) diluted at 1:2000. Human umbilical vein endothelial cells (HUVECs), cultured in supplemented EGM-2 culture medium (Cambrex, Walkersville, MD, USA) on 24-well plates, were harvested with sample buffers. Similarly, the blotted membranes were incubated with a polyclonal anti-ChAT antibody (Millipore) diluted at 1:500, which detects several bands with a M.W. of 68 - 70kDa. Each antibody was used in conjunction with a horseradish peroxidase-conjugated secondary antibody. For *in vitro* studies, each experiment was independently performed 3 times. After that, the densitometry analysis was performed.

Reverse transcription-polymerase chain reaction (RT-PCR)

Total RNA was extracted from cells, and total RNA (1 μg) was reverse-transcribed to obtain single-stranded cDNA using a kit. Specific human cholinergic receptor primers were designed according to previous studies [17, 18]. PCR amplification was performed with 40 cycles of the reaction and annealing temperatures of 60ºC. Primer sequences were as follows:

m1, TGAGGGCTCACCAGAGACT (forward),
GTCCAGGTGAGGATGAAGG (reverse);
m2, ACAAGGAAGGATAGTGAAGCC (forward),
CATCTCCATTCTGACCTGAAG (reverse);
α4, CTCACCGTCCTTCTGTGTC (forward),
CTGGCTTTCTCAGCTTCCAG (reverse);
α7, AGGCCACCTCATCAGCAG (forward),
GTACGCTGGTTTCCCTTTGA (reverse);
GAPDH, CGTCTTCACCACCATGGAGA (forward),
CGGCCATCACGCCACAGCTT (reverse).

Cell culture

HUVECs or human aorta endothelial cells (HAECs) were cultured in EGM-2 culture medium (Cambrex), supplemented with heparin, IGF-I, VEGF, bFGF, EGF, hydrocortisone, FBS, and ascorbic acid, according to the manufacturer's instruction. The final concentration of each reagent was as follows: 1 μM of donepezil (Eisai Co., Ltd., Tokyo, Japan), 0.1 μM of nicotine, which has been reported to possess angiogenic property [11-13], and 100 μM of ACh (Sigma-Aldrich, St. Louis, MO, USA).

To investigate the effects on tube formation, *in vitro* angiogenesis, HUVECs were cultured on Matrigel with complete growth factors (Becton Dickinson Labware, Bedford, MA, USA) using 96-well plates. HUVECs (1×10^4 cells) were seeded on Matrigel (50%)-coated wells and incubated for 24 h in DMEM with 20% FBS, 25 μg/ml endothelial cell growth supplement (Upstate, Lake Placid, NY, USA), 10 U/ml heparin and any one of the study agents. The number of tubes per low power field in each well was counted and compared.

MTT activity

To evaluate HUVEC proliferation, we measured the reduction activity of 3-(4,5-dimethylthiazol-2-yl)-2,5-diphenyl tetrazolium bromide (MTT). One hour before sampling, MTT reagents (10 μL) were added to the culture medium (100 μL), incubated, and the absorbance at 450 nm was measured (Cell Counting Kit-8; Dojindo, Kumamoto, Japan), according to the manufacturer's protocol.

Caspase 3/7 activity

According to the manufacturer's protocol (Promega, Madison, WI, USA), HUVECs treated with or without donepezil were cultured with an equal volume of Caspase-Glo 3/7 reagent for 3 h, followed by measuring the luminescence of each sample using the luminometer manufacturer's protocol.

Statistical analysis

The data are presented as means ± S.E. The mean values between the 2 groups were compared using the unpaired Student's *t*-test. Differences among data for the in vitro studies were assessed by the Kruskal-Wallis test for multiple comparisons, followed by Scheffe's post-hoc test. Differences were considered significant at $P < 0.05$.

Results

Donepezil activates angiogenic signals and accelerates tube formation *in vitro*.

Donepezil transduces angiogenic signals. In the normoxic condition, donepezil (1 μM) elevated the HIF-1α protein level, and then augmented expression of VEGF and activated phosphorylation of Flk-1, VEGF type 2 receptor (Figure 1A), which composes critical angiogenic signaling. Correspondingly, donepezil enhanced tube formation (Figure 1B) in HUVECs within 24 h (12.8 ± 0.6 in donepezil-treated HUVECs vs. 6.7 ± 0.4 in control, $P < 0.01$), suggesting that donepezil is capable of accelerating angiogenesis. This effect of donepezil was inhibited by the muscarinic receptor antagonist atropine (100 μM) (0.7 ± 0.2, $P < 0.01$) and the selective α7 nicotinic receptor antagonist α-bungarotoxin (0.1 μM) (2.0 ± 0.6, $P < 0.01$) (Figure 1B).

The mechanisms of donepezil-induced acceleration of angiogenesis were revealed by the effect of ACh and nicotine, which have been reported to promote angiogenesis [11-13], on HUVECs. ACh and nicotine shared the same angiogenic signals (Figure 1C). Moreover, ACh accelerated HUVEC tube formation within 24 h (16.8 ± 0.9 with 100 μM of ACh vs. 7.3 ± 0.5 control, $P < 0.01$) (Figure 1D); however, it was markedly suppressed by atropine (100 μM) (2.8 ± 0.8, $P < 0.01$) and α-bungarotoxin (0.1 μM) (2.7 ± 0.6, $P < 0.01$) (Figure1D). Similarly, ACh accelerated tube formation in HAECs, which was partially suppressed by atropine (data not shown). These results suggest that ACh promotes *in vitro* angiogenesis through angiogenic signal transduction and that the signal is mediated via both nicotinic and muscarinic receptors.

Donepezil promotes angiogenesis and suppresses ischemia-induced muscular atrophy in a murine hindlimb ischemia model

In untreated WT, muscular atrophy of the left quadriceps femoris muscle was evident within 4 weeks after hindlimb ischemia due to femoral artery ligation (Figure 2A, arrowheads in the left panel). The temperature in the left ischemic limb increased gradually during the follow-up; however, it did not comparably recover to the level of the contralateral hindlimb (Figure 2B). The ratio of skin temperature in the left hindlimb to that in the right hindlimb, the laterality in temperature, decreased to 0.50 ± 0.04 soon after ligation, followed by an elevation to 0.81 ± 0.02. In contrast, donepezil-treated mice did not suffer from severe muscular atrophy (Figure 2A). The weight ratio of the left hindlimb to the right was 1.02 ± 0.04 ($P < 0.05$, n = 10) in donepezil-treated mice, compared with 0.85 ± 0.01 (n = 10) in control untreated mice (Figure 2A). Furthermore, the laterality of temperature increased to 0.95 ± 0.01 with donepezil treatment ($P < 0.01$

vs. control) (Figure 2B). A pathological study revealed that, compared to untreated muscle (left in control, Figure 2C), the number of nuclei in treated muscle increased along with more capillary-like structures (Figure 2C). The number of nuclei per field in the donepezil-treated left hindlimb increased significantly compared to that in non-treated and ischemic hindlimbs (17.8 ± 1.4 vs. 8.6 ± 0.9, $P < 0.01$, n = 9). The immunohistochemical study showed that cells positive for VEGF immunoreactivity were sparsely detected in the control. In contrast, dense VEGF signals were detected in the donepezil-treated muscle coincidence with small capillaries (Figure 2C). Western blot analysis showed that the expression of both HIF-1α (318.4 ± 29.9 vs. 100.0 ± 6.7 in the control, $P < 0.01$, n = 9) and VEGF (144.5 ± 2.9 vs. 99.8 ± 9.9 in the control, $P < 0.01$, n = 9) in the left hindlimbs from donepezil-treated mice were higher than that in the left hindlimbs from the control (Figure 2C).

These effects of donepezil were also evaluated using α-bungarotoxin, mecamylamine, and atropine (Figure 2D). VEGF protein expression in the left hindlimb was elevated by donepezil ($P < 0.05$); however, donepezil treatment combined with α-bungarotoxin did not suppress VEGF expression. Mecamylamine and atropine showed a trend toward reduced VEGF expression, but could not diminish it completely (not significant vs. donepezil). Similarly, PCNA expression was elevated by donepezil ($P < 0.01$), the level of which was not diminished by α-bungarotoxin ($P < 0.05$); however, mecamylamine ($P < 0.05$ vs. donepezil) and atropine ($P < 0.01$ vs. donepezil) blunted PCNA expression. The VEGF and PCNA immunoreactive signals were especially localized at endothelial cells (Figure 2E). Endothelial cells with both VEGF- and PCNA-positive signals were evident in left hindlimbs of donepezil-treated mice, compared to that in controls. The protein level of cleaved caspase-3, an indicator of caspase-3 activation, was drastically reduced by donepezil ($P < 0.05$), but was not affected by α-bungarotoxin, mecamylamine or atropine (not significant vs. donepezil). Furthermore, the laterality of temperature sustained by donepezil did not diminish with each antagonist ($P < 0.01$ vs. control, but not significant vs. donepezil) (Figure 2F). These results suggest that donepezil activates angiogenesis in a hindlimb ischemia model with upregulated angiogenic factors, enhanced proliferation, inhibition of apoptosis, and suppressed ischemia-induced muscular atrophy; however, partly not through already known cholinergic receptors.

Angiography with ICG revealed a marked increase in perfusion with donepezil treatment, which was comparable to the non-ischemic contralateral limb (1.08 ± 0.6 and 1.00 ± 0.84 vs. 0.74 ± 0.27, $P < 0.01$). Furthermore, a blood flow assay using fluorescent microspheres revealed that donepezil enhanced blood flow recovery (124.9

± 15.8 in donepezil vs. 59.0 ± 12.2 in control, $P < 0.05$, n = 5 in each) (Figure 2G), suggesting that donepezil functionally recovered tissue perfusion in the ischemic hindlimb.

Donepezil accelerates angiogenesis even in α7 KO with hindlimb ischemia

Previous reports using α7 KO indicated that a nicotinic receptor is responsible for angiogenesis [11-13]. Therefore, to investigate whether the angiogenic effects of donepezil are mediated through α7 nicotinic receptors, we studied the effects of donepezil on peripheral limb ischemia using these mice. Compared with control untreated α7 KO (0.93 ± 0.02, n = 13), donepezil-treated α7 KO surprisingly attenuated ischemia-induced muscular atrophy with a leg-weight ratio of 1.01 ± 0.04 ($P < 0.01$, n = 13) (Figure 3A). ICG angiography revealed that tissue perfusion in the left hidlimb was sustained in donepezil-treated α7 KO (1.23 ± 0.10 vs. 0.70 ± 0.27 in control, $P < 0.01$), as supported by the microsphere assay (117.4 ± 9.7 vs. 70.4 ± 10.7 in control, $P < 0.05$, n = 5 in each) (Figure 3B). VEGF expression in quadriceps femoris muscle from donepezil-treated α7 KO was more elevated (191.4 ± 10.0 vs. 100 ± 1.3 in control, $P < 0.01$) (Figure 3C) and the increased immunoreactivity was also detected in the treated muscle. Finally, donepezil accelerated temperature recovery in ischemic hindlimbs (Figure 3D). Compared with the laterality in temperature in WT 4 weeks after ligation, that in α7 KO decreased further to 0.71 ± 0.03 (vs. 0.81 ± 0.02 in WT, $P < 0.05$); however, treatment with donepezil elevated the ratio to 0.98 ± 0.02 even in α7 KO ($P < 0.01$).

The lower dose of donepezil, 0.083 mg/kg/day, which is comparable to that used in clinical settings, was also effective for accelerating *in vivo* angiogenesis (the laterality in temperature 0.96 ± 0.04, $P < 0.01$) (Figure 3E). Taken with the *in vivo* data using α-bungarotoxin, these results also suggest that donepezil rescues ischemic hindlimbs independent of the α7 nicotinic receptor.

Donepezil augments VEGF expression in the heart and ChAT protein expression in endothelial cells

In addition to the ischemic hindlimbs, donepezil also enhanced VEGF signals in the WT heart, compared to untreated WT (Figure 4A), as supported by Western blot analysis (181.8 ± 4.2% vs. 100.0 ± 0.6% in control, $P < 0.01$). Similar donepezil effects on VEGF production in the heart were observed in α7 KO (Figure 4B). Compatible with VEGF immunoreactivity in the hindlimb, the immunohistochemical study with the anti-VEGF antibody showed positive signals with capillary-like appearance in the heart

(Figure 4A, 4B).

HUVECs were treated with 1 μM donepezil to study whether donepezil modulates ACh synthesis in endothelial cells. Donepezil elevated choline acetyltransferase (ChAT) protein expression in HUVECs (248.2 ± 3.1% vs. 100.0 ± 11.0% in control, $P < 0.01$) (Figure 4C). Because ChAT is a crucial enzyme for ACh synthesis, this suggests that donepezil regulates ACh level in endothelial cells. During treatment with donepezil, cholinergic receptor mRNAs in HUVECs were also upregulated. RT-PCR showed that m2, α4, and α7 mRNA expression were increased by donepezil, compared with α3 and GAPDH mRNA expression (Figure 4D). Furthermore, in HUVECs treated with donepezil for 24 h, caspase 3/7 activity was suppressed when apoptosis was induced by growth factor withdrawal (69.3 ± 3.8 % vs. control, $P < 0.01$, n = 6) (Figure 4E). In contrast, donepezil showed only a trend toward increased MTT activity. Taken with the *in vivo* results, these in vitro data suggest that donepezil plays a role in inhibiting apoptosis and accelerating proliferation.

Discussion

The present study indicates 2 novel and critical points involved in an angiogenesis regulating system. First, ACh possessed angiogenic effects on endothelial cells, with increased HIF-1α expression, followed by elevated VEGF expression and accelerated tube formation, suggesting that ACh modulates intrinsic angiogenesis-responsible machinery in endothelial cells. Second, donepezil enhanced angiogenesis by activating the similar machinery. Specifically, donepezil activated protein expression of VEGF and ChAT, a critical enzyme for *de novo* ACh synthesis, accelerated endothelial cell proliferation, and inhibited apoptosis, partly independent of cholinergic receptors. These results suggest that donepezil regulates angiogenesis through a non-hypoxic HIF-1α induction pathway, which might be triggered by increased ACh [3,4].

Donepezil was developed to treat patients with Alzheimer's disease as an acetylcholinesterase inhibitor [12,13]. Donepezil prevents neurons from apoptosis and degeneration [19-22] and improves cognitive abilities in patients with Alzheimer's disease [23-25]. However, only few studies have focused on the angiogenesis accelerating effects of donepezil [26]. Thus, the present study suggests a novel mechanism by which donepezil improves cognitive performance in these patients through acceleration of angiogenesis.

Our previous study demonstrated that ACh triggers a cell survival signal pathway and transactivates HIF-1α-regulated downstream genes, preventing cells from hypoxia-induced apoptosis [3]. This prompted us to speculate that cholinergic stimuli also possess angiogenesis-promoting effects. ACh clearly promoted angiogenesis and acceleration of tube formation; however, it is quite difficult to apply ACh directly to an *in vivo* model, because ACh evokes life threatening side effects, i.e., bronchospasm, enhanced secretion, and diarrhea [27,28]. Therefore, instead of ACh, we selected donepezil, which is globally used in clinical settings without side effects and has been demonstrated to increase tissue ACh levels [9,10,21]. As expected, donepezil promoted angiogenesis *in vitro* and concomitantly activated the HIF-1α/VEGF pathway. These effects of donepezil were also confirmed *in vivo*. Orally administered donepezil remarkably increased VEGF and PCNA immunoreactivity in endothelial cells of WT ischemic left quadriceps femoris muscles, indicating that donepezil activates angiogenesis by upregulating angiogenic signals in endothelial cells. To further study whether the effect of donepezil on endothelial cells is dependent on cholinergic receptors, donepezil treatment was conducted in the presence of each cholinergic receptor antagonist. Unexpectedly, *in vivo* angiogenesis was not clearly blunted by the

antagonists, especially in terms of inhibiting apoptosis. α-Bungarotoxin, a selective α7 nicotinic receptor antagonist, did not inhibit apoptosis or expression of the angiogenic factors VEGF and PCNA, suggesting that donepezil plays an angiogenic role in endothelial cells independent of α7 nicotinic receptors. This result was also confirmed using α7 KO.

In this study, we used α7 KO to evaluate the *in vivo* angiogenic effects of donepezil. The studies by Cooke JP et al. utilizing α7 KO indicated that nicotine plays a crucial role in angiogenesis [11-13]. They demonstrated an impaired angiogenic effect of nicotine in α7 KO [12]. However, except for the α7 nicotinic receptor, there have been no studies investigating the role of cholinergic receptors involved in angiogenesis. Only α7 KO are available for angiogenesis studies; therefore, we selected them for the present study. Our results partially contrasted with Cooke's *in vitro* studies because the ACh effects were moderately blocked by both α-bungarotoxin and atropine, suggesting that the effects of ACh are mediated by 2 receptors, i.e., a nicotinic receptor and a muscarinic receptor. This discrepancy might be derived from different HUVEC sources used in the studies. We investigated the effects of donepezil using α7 KO expecting that the angiogenic effects of donepezil would be blunted. However, donepezil exhibited the angiogenesis-accelerating effect even in α7 KO. This result was also compatible with that of WT treated with donepezil and α-bungarotoxin. Taken with the WT results, this suggests that donepezil directly activates the angiogenic machinery and proliferation potency in endothelial cells, leading to inhibition of apoptosis, independent of α7 nicotinic receptors.

Because donepezil not only inhibits acetylcholinesterase but also upregulates ChAT, it was expected that the intracellular ACh level might be increased. However, even using HPLC, ACh levels could not be detected in endothelial cells, although we have thus far succeeded in measuring intracellular ACh levels of other cells, such as HEK293 cells, H9c2 cells, and primary rat cardiomyocytes [29]. This does not exclude the possibility that endothelial cells cannot synthesize ACh. As shown in this study, expression of other subtypes of cholinergic receptors, such as m2, α4, and α7, was upregulated by donepezil. This effect might also contribute to accelerated angiogenesis in α7 KO. The effects of donepezil on *in vivo* angiogenesis were also observed with a low dose, which is compatible with a clinical setting. Our preliminary study has already confirmed that a high dose of donepezil has no significant effects on murine heart rate or blood pressure. Therefore, it is suggested that low dose donepezil exerts angiogenic effect independent of hemodynamic effects.

Kawashima and Wessler [30,31] speculated that non-neuronal and non-central cells

synthesize ACh. Our recent study has demonstrated for the first time that cardiomyocytes also possess the intracellular ACh synthesis system, which is transcriptionally activated in a positive feedback manner, and donepezil also elevates ACh level in cardiomyocytes, which was partly independent of muscarinic receptors [29]. These findings also suggest that donepezil exerts its own effects partly independent of cholinergic receptors. On the basis of previous studies by Cooke, who did not clearly mention an ACh source, together with our recent study [29], it is suggested that systemically administered donepezil modulates ACh levels in various cells through a cholinergic receptor-dependent or -independent manner, and ACh derived from such cells might play a key role in angiogenesis.

Although donepezil is an acetylcholinesterase inhibitor, a lack of information on its receptor and action mechanisms makes our results difficult to interpret. Therefore, it is speculated that other mechanisms, i.e., a pathway other than acetylcholinesterase inhibition, might be involved in the angiogenesis-accelerating effects, and donepezil might directly bind to endothelial cell receptors not yet identified. This remains to be clarified.

In conclusion, we have presented a novel concept that donepezil possesses angiogenic properties through enhanced proliferation, increased angiogenic factor expression, and inhibition of apoptosis.

Acknowledgement

This study was supported by a Grant-in-Aid for Scientific Research from Japan Society for the Promotion of Science (19590251).

.

References

1. Li M, Zheng C, Sato T, Kawada T, Sugimachi M, Sunagawa K. Vagal nerve stimulation markedly improves long-term survival after chronic heart failure in rats. Circulation 2004;109:120-124.

2. Ando M, Katare RG, Kakinuma Y, Zhang D, Yamasaki F, Muramoto K, Sato T. Efferent vagal nerve stimulation protects heart against ischemia-induced arrhythmias by preserving connexin43 protein. Circulation 2005;112:164-170.

3. Kakinuma Y, Ando M, Kuwabara M, Katare RG, Okudela K, Kobayashi M, Sato T. Acetylcholine from vagal stimulation protects cardiomyocytes against ischemia and hypoxia involving additive non-hypoxic induction of HIF-1alpha. FEBS Lett 2005;579:2111-2118.

4. Kuwabara M, Kakinuma Y, Ando M, Katare RG, Yamasaki F, Doi Y, Sato T. Nitric oxide stimulates vascular endothelial growth factor production in cardiomyocytes involved in angiogenesis. J Physiol Sci 2006;56:95-101.

5. Zhao X, Lu X, Feng Q. Deficiency in endothelial nitric oxide synthase impairs myocardial angiogenesis. Am J Physiol Heart Circ Physiol 2002;283:H2371-2378.

6. Ng QS, Goh V, Milner J, Stratford MR, Folkes LK, Tozer GM, Saunders MI, Hoskin PJ. Effect of nitric-oxide synthesis on tumour blood volume and vascular activity: a phase I study. Lancet Oncol 2007;8:111-118.

7. Williams JL, Cartland D, Hussain A, Egginton S. A differential role for nitric oxide in two forms of physiological angiogenesis in mouse. J Physiol 2006;570:445-454.

8. Ridnour LA, Isenberg JS, Espey MG, Thomas DD, Roberts DD, Wink DA. Nitric oxide regulates angiogenesis through a functional switch involving thrombospondin-1. Proc Natl Acad Sci U S A 2005;102:13147-13152.

9. Bohnen NI, Kaufer DI, Hendrickson R, Ivanco LS, Lopresti BJ, Koeppe RA, Meltzer CC, Constantine G, Davis JG, Mathis CA, Dekosky ST, Moore RY. Degree of inhibition of cortical acetylcholinesterase activity and cognitive effects by donepezil treatment in Alzheimer's disease. J Neurol Neurosurg Psychiatry 2005;76:315-319.

10. Hatip-Al-Khatib I, Iwasaki K, Yoshimitsu Y, Arai T, Egashira N, Mishima K, Ikeda T, Fujiwara M. Effect of oral administration of zanapezil (TAK-147) for 21 days on acetylcholine and monoamines levels in the ventral hippocampus of freely moving rats. Br J Pharmacol 2005;145:1035-1044.

11. Heeschen C, Jang JJ, Weis M, Pathak A, Kaji S, Hu RS, Tsao PS, Johnson FL, Cooke JP. Nicotine stimulates angiogenesis and promotes tumor growth and atherosclerosis.
Nat Med 2001;7:833-839.

12. Heeschen C, Weis M, Aicher A, Dimmeler S, Cooke JP. A novel angiogenic pathway mediated by non-neuronal nicotinic acetylcholine receptors. J Clin Invest 2002;110:527-536.

13. Heeschen C, Weis M, Cooke JP. Nicotine promotes arteriogenesis. J Am Coll Cardiol 2003;41:489-496.

14. Li X-W, Wang H. Non-neuronal nicotinic alpha7 receptor, a new endothelial target for revascularization. Life Sci 2006;78:1863-1870.

15. Cardinal TR, Hoying JB. A modified fluorescent microsphere-based approach for determining resting and hyperemic blood flows in individual murine skeletal muscles. Vascular Pharmacol 2007;47:48-56.

16. Hodeige D, de Pauw M, Eechaute W, Weyne J, Heyndrickx GR. On the validity of blood glow measurement using colored microspheres. Am J Physiol Heart Circ Physiol 1999;276:H1150-1158.

17. Elhusseiny A, Cohen Z, Olivier A, Stanimirović DB, Hamel E. (1998) Functional acetylcholine muscarinic receptor subtypes in human brain microcirculation: identification and cellular localization. J Cereb Blood Flow Metab 1998;19:794-802.

18. Lips KS, Bruggman D, Pfeil U, Vollerthun R, Grando SA, Kummer W. Nicotinic acetylcholine receptors in rat and human placenta. Placenta 2005;26:735-746.

19. Takada Y, Yonezawa A, Kume T, Katsuki H, Kaneko S, Sugimoto H, Akaike A. Nicotinic acetylcholine receptor-mediated neuroprotection by donepezil against glutamate neurotoxicity in rat cortical neurons. J Pharmacol Exp Ther 2003;306:772-777.

20. Kimura M, Komatsu H, Ogura H, Sawada K. Comparison of donepezil and memantine for protective effect against amyloid-beta(1-42) toxicity in rat septal neurons. Neurosci Lett 2005;391:17-21.

21. Kasa P, Papp H, Kasa P Jr, Torok I. Donepezil dose-dependently inhibits acetylcholinesterase activity in various areas and in the presynaptic cholinergic and the postsynaptic cholinoceptive enzyme-positive structures in the human and rat brain. Neuroscience 2000;101:89-100.

22. Ginestet L, Ferrario JE, Raisman-Vozari R, Hirsch EC, Debeir T. Donepezil induces a cholinergic sprouting in basocortical degeneration. J Neurochem 2007;102:434-440.

23. Rogers SL, Doody RS, Mohs RC, Friedhoff LT. Donepezil improves cognition and global function in Alzheimer disease: a 15-week, double-blind, placebo-controlled study. Donepezil Study Group. Arch Intern Med 1998;158:1021-1031.

24. Feldman H, Gauthier S, Hecker J, Vellas B, Xu Y, Ieni JR, Schwam EM; Donepezil MSAD Study Investigators Group. Efficacy and safety of donepezil in patients with more severe Alzheimer's disease: a subgroup analysis from a randomized, placebo-controlled trial. Int J Geriatr Psychiatry 2005;20:559-569.

25. Gauthier S, Feldman H, Hecker J, Vellas B, Emir B, Subbiah P; Donepezil MSAD Study Investigators' Group. Functional, cognitive and behavioral effects of donepezil in patients with moderate Alzheimer's disease. Curr Med Res Opin 2002;18:347-354.

26. Shimizu S, Hanyu H, Iwamoto T, Koizumi K, Abe K. SPECT follow-up study of cerebral blood flow changes during Donepezil therapy in patients with Alzheimer's disease. J Neuroimaging 2006;16:16-23

27. Fryer AD, Jacoby DB Muscarinic receptors and control of airway smooth muscle. Am J Respir Crit Care Med 1998;185: S154-S160.

28. Kavirajan H, Schneider LS. Efficacy and adverse effects of cholinesterase inhibitors and memantine in vascular dementia: a meta-analysis of randomised controlled trials. Lancet Neurol 2007;6:782-792.

29. Kakinuma Y, Akiyama T, Sato T. Cholinoceptive and cholinergic properties of cardiomyocytes involving an amplification mechanism for vagal efferent effects in sparsely innervated ventricular myocardium. FEBS J. 2009;276:5111-5125.

30. Fujii T, Tsuchiya T, Yamada S, Fujimoto K, Suzuki T, Kasahara T, Kawashima K. Localization and synthesis of acetylcholine in human leukemic T cell lines. J Neurosci Res 1996;44:66-72.

31. Klapproth H, Reinheimer T, Metzen J, Munch M, Bittinger F, Kirkpatrick CJ, Hohle KD, Schemann M, Racke K, Wessler I. Non-neuronal acetylcholine, a signalling molecule synthezised by surface cells of rat and man. Naunyn Schmiedebergs Arch Pharmacol 1997;355:515-523.

Figure legends

Figure 1

Donepezil mediates angiogenic signals in HUVECs to activate tube formation.

(A) Donepezil (1 μM) increased the HIF-1α protein expression level during normoxic conditions. This induction of HIF-1α was followed by increased VEGF expression and activated phosphorylation of the VEGF receptor-2 Flk-1 in HUVECs (n = 3). (B) Donepezil also accelerated tube formation in HUVECs (12.8 ± 0.6 tube number per field vs. 6.7 ± 0.4 in control, $P < 0.01$, n = 3). In contrast, donepezil-induced tube formation was inhibited by atropine (100 μM) or α-bungarotoxine (0.1 μM). Scale bar represents 50 μm. Representative data from 3 experiments are shown for each study. (C) ACh (100 μM) and nicotine (0.1 μM) increased HIF-1α and VEGF protein expression. (D) Tube formation in untreated HUVECs progressed within 24 h, and ACh markedly accelerated tube formation. ACh (100 μM) accelerated tube formation (16.8 ± 0.9 in 100 μM of ACh vs. 7.3 ± 0.5, $P < 0.01$, n = 3). ACh-induced acceleration of tube formation was partly suppressed by atropine (100 μM) (2.8 ± 0.8, $P < 0.01$, n = 3) and α-bungarotoxine (0.1 μM) (2.7 ± 0.6, $P < 0.01$, n = 3). Scale bars represent 100 μm. Representative data from 3 experiments are shown for each study (D).

Figure 2

Donepezil promotes angiogenesis in C57 BL6/J wild-type mice (WT) suffering from left hindlimb ischemia and suppresses ischemia-induced muscular atrophy and reduction of skin temperature.

(A) WT treated with orally administered donepezil showed comparable muscular volume between the right and left hindlimb, even with the left hindlimb ischemia (arrowheads in the right panel), compared with untreated WT mice (arrowheads in the left panel) (n = 10). (B) Donepezil accelerated skin temperature recovery in the left hindlimb within 4 weeks and sustained the skin temperature comparably to the right hindlimb. The ratio of skin temperature in the left hindlimb to the right, the laterality in the temperature, was increased by donepezil from 0.50 ± 0.04 after ligation to 0.95 ± 0.01 (vs. 0.81 ± 0.01 in control, $P < 0.01$, n = 10). (C) Compatible with this, donepezil-treated WT mice demonstrated more nuclei aligned with a vasculature-like appearance, especially in the left ischemic hindlimb (the right panel in donepezil, Figure 2C). Magnification: ×200. Numbers of nuclei per visual field in the donepezil-treated left ischemic hindlimb increased significantly compared to the non-treated hindlimb ($P < 0.01$, n = 9). VEGF immunoreactivity was upregulated by donepezil in the left

ischemic hindlimb (the right panel in Figure 2C) compared with the control. Scale bars represent 50 μm. HIF-1α and VEGF protein expression in the left quadriceps femoris muscle increased significantly in donepezil-treated WT ($P < 0.01$, n = 9). (D) This effect of donepezil on VEGF signals did not significantly decrease following α-bungarotoxin, mecamylamine, or atropine treatment. Inhibition of caspase-3 by donepezil was also not attenuated by cholinergic antagonists. The PCNA expression level was elevated by donepezil, but not reduced by α-bungarotoxin. (E) Donepezil increased VEGF and PCNA immunoreactivity, specifically in endothelial cells, whereas α-bungarotoxin did not affect VEGF- and PCNA-positive endothelial cells, as shown in the Western blot analysis. (F) Sustained skin temperature by donepezil was not blunted by α-bungarotoxin, mecamylamine, or atropine ($P < 0.01$ vs. control, respectively). (G) ICG angiography revealed comparable tissue perfusion between the right and left hindlimbs in donepezil-treated WT (1.00 ± 0.84 vs. 1.08 ± 6.1; not significant, NS, n = 3) (arrowheads in the right panel). In contrast, untreated WT mice showed lower tissue perfusion in the left hindlimb (0.74 ± 0.27 vs. 1.00 ± 0.43, $P < 0.01$, n = 3) (arrowheads in the left panel). Representative ICG angiography data from 3 experiments are presented. A microsphere assay also showed increased blood flow in donepezil-treated hindlimbs, evaluated with the ratio of left to right fluorescent signals (115.4 ± 19.3 in donepezil vs. 75.2 ± 7.5 in control, $P < 0.05$, n = 5).

Figure 3

Donepezil exhibits comparable angiogenic effects in the ischemic hindlimb model using α7 KO mice.

(A) Donepezil inhibited ischemia-induced muscular atrophy in α7 KO. The ratio of the left leg weight to the right leg weight in donepezil-treated mice increased compared with untreated mice (n = 13). (B) ICG angiography showed that donepezil attenuated ischemia-induced impairment of tissue perfusion (1.23 ± 0.10 vs. 0.70 ± 0.27, $P < 0.01$, n = 3) compared to untreated α7 KO. Representative ICG angiography data from 3 experiments are presented. Using a microsphere assay, donepezil inhibited the reduction of blood flow (117.4 ± 9.7 vs. 70.4 ± 10.7 in control, $P < 0.05$, n = 5 in each). (C) VEGF protein expression in the left ischemic hindlimb of donepezil-treated α7 KO increased compared with untreated α7 KO ($P < 0.01$, n=11). More intense VEGF immunoreactivity was detected in donepezil-treated α7 KO, especially between each muscle fiber. Scale bar represents 50 μm. (D) Recovery of skin temperature in the left ischemic hindlimb of donepezil-treated α7 KO was more accelerated during the treatment (arrowheads in the lower panel). The laterality in temperature in α7 KO (0.71

± 0.03), which was lower than that in WT (0.81 ± 0.02), increased with donepezil (0.98 ± 0.02, $P < 0.01$, n = 13). In contrast, untreated α7 KO showed poor skin temperature recovery (arrowheads in the upper panel). (E) Donepezil, even at a lower dose, inhibited the reduction in skin temperature in the left ischemic hindlimb (arrowheads in the lower panel), as evidenced by the elevation of laterality in temperature (0.96 ± 0.04, $P < 0.01$, n = 9).

Figure 4

Donepezil increases VEGF expression in the heart.

(A) VEGF immunoreactivity was more in the heart of donepezil-treated WT than in that of untreated WT. Scale bars represent 50 μm. Cardiac expression of the VEGF protein was more enhanced by donepezil ($P < 0.01$, n = 9). (B) More VEGF-positive signals were also detected in donepezil-treated α7 KO than in untreated α7 KO. A magnified view is shown in (A) and (B), which demonstrates the capillary-like appearance. Scale bars represent 50 μm. (C) Donepezil (1 μM) increased ChAT protein expression in HUVECs within 10 h, ($P < 0.01$, n = 6). (D) mRNA expression of m2, α4, and α7 in HUVECs increased with donepezil within 24 h. In contrast, both α3 and GAPDH mRNA expression was not elevated. (E) Caspase 3/7 activity decreased significantly with a 24 h donepezil treatment (1 μM) in the case of depletion of growth factors (69.3 ± 3.8 % vs. control, $P < 0.01$, n = 6); however, MTT activity was not affected by donepezil (NS).

Kakinuma Y. et al.
Figure 1

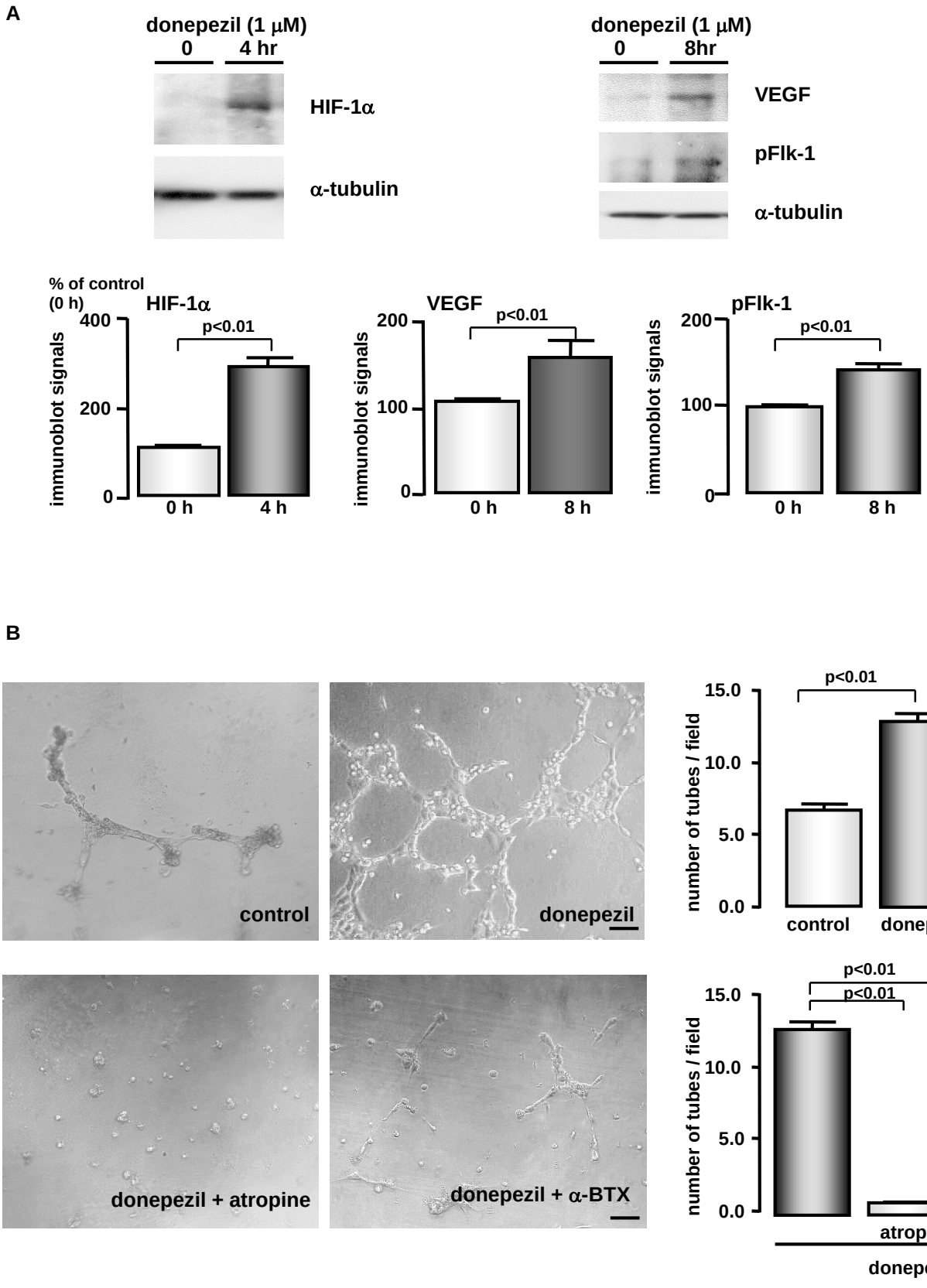

Kakinuma Y.
Figure 1

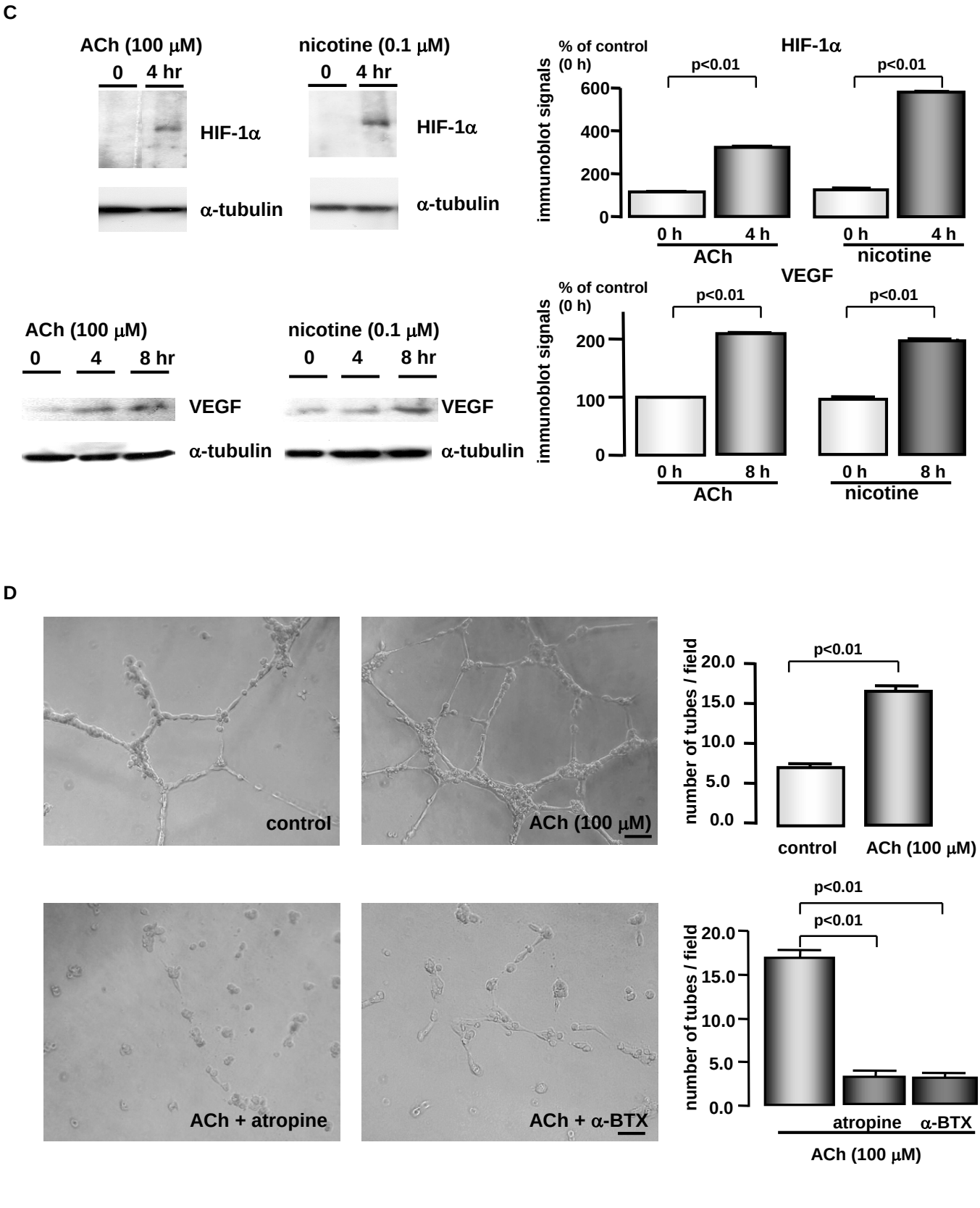

Kakinuma Y
Figure 2

A

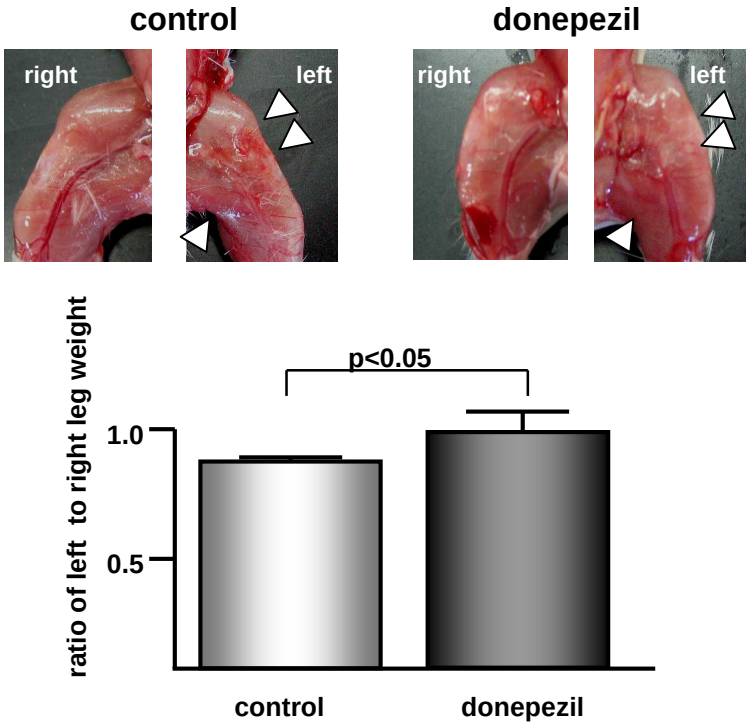

B

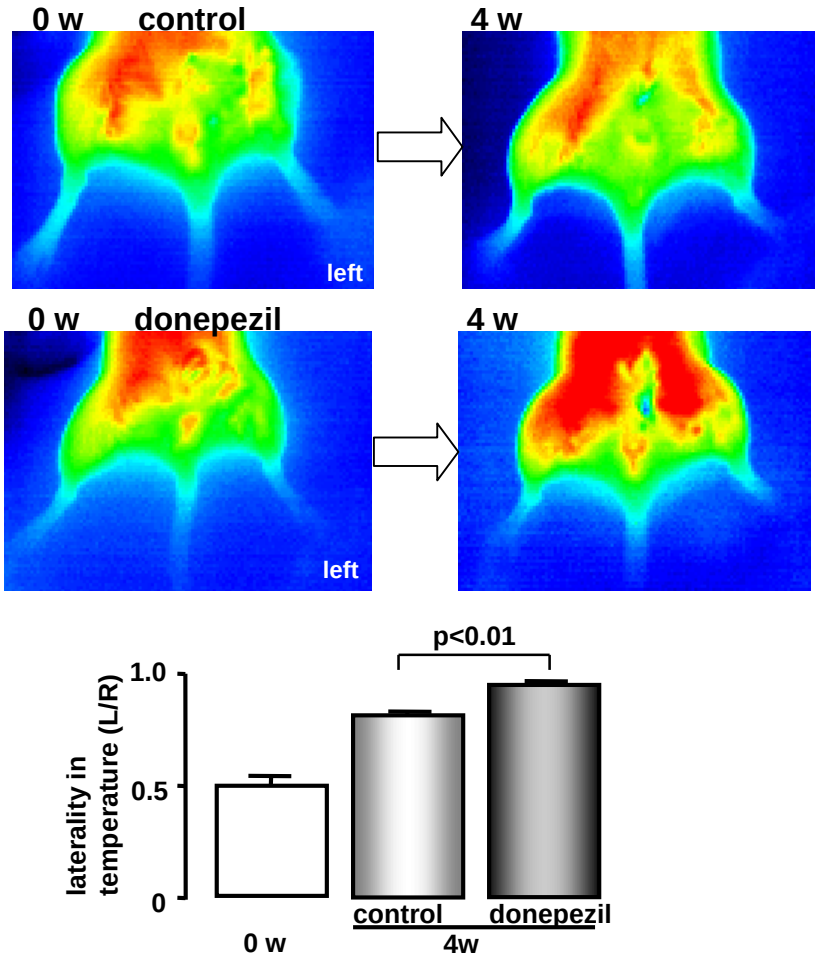

Kakinuma Y. et al.
Figure 2

C

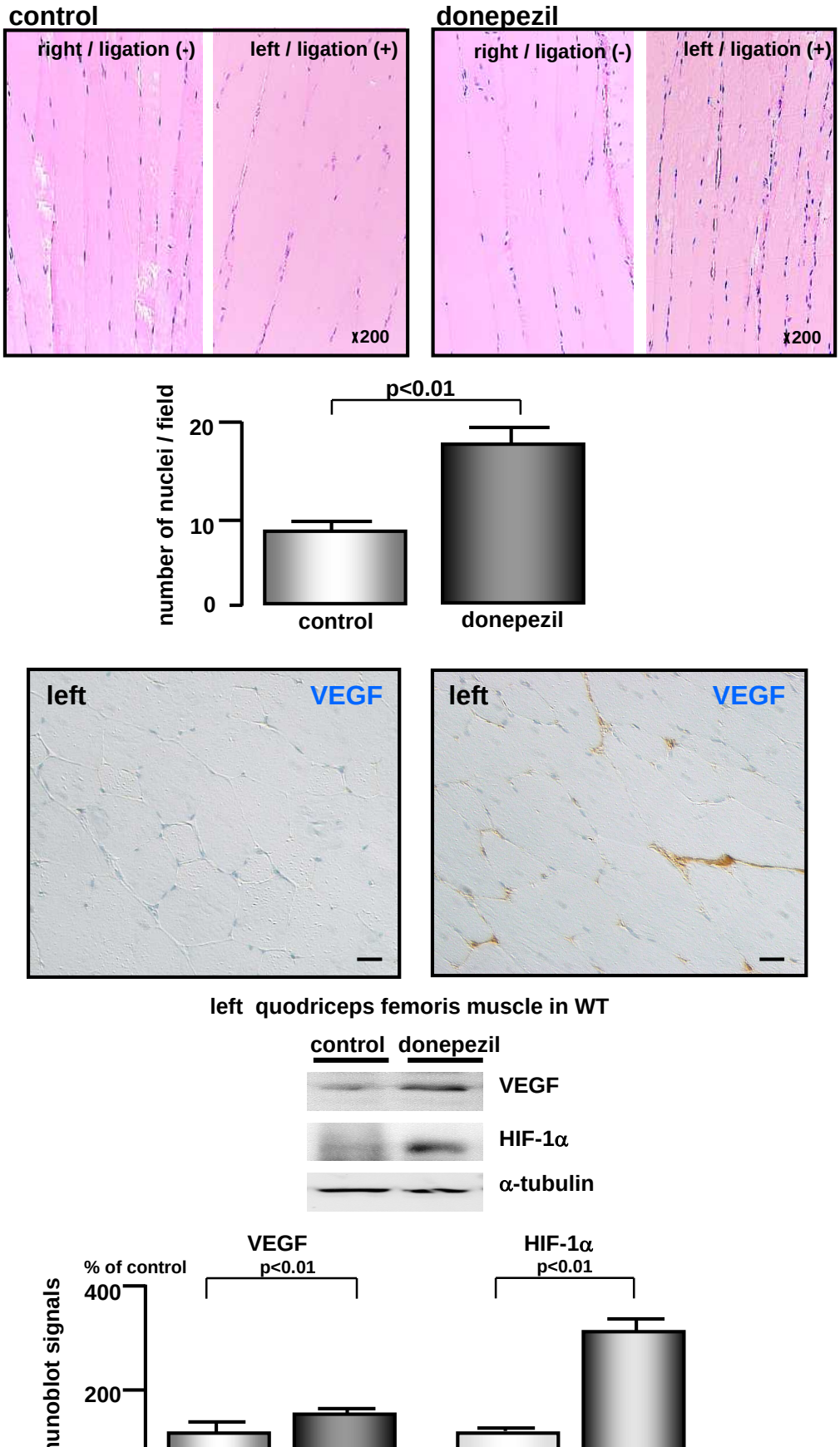

Kakinuma Y. et al.
Figure 2

D

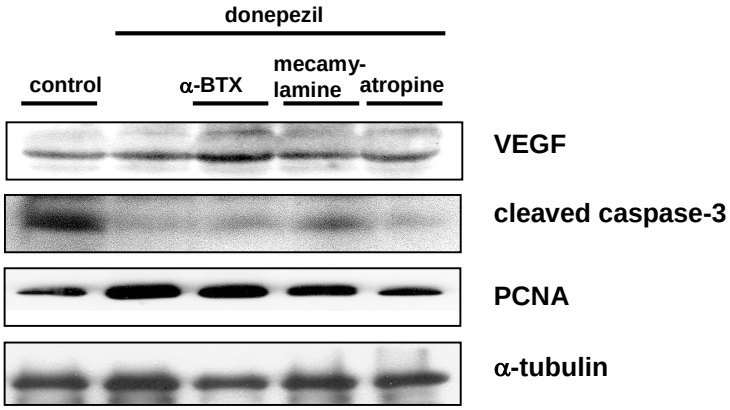

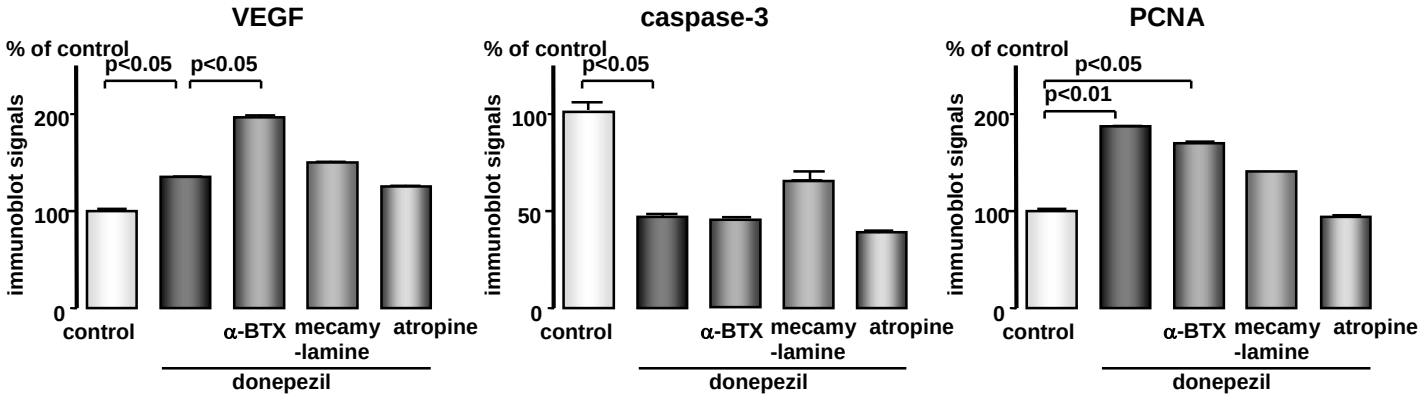

E

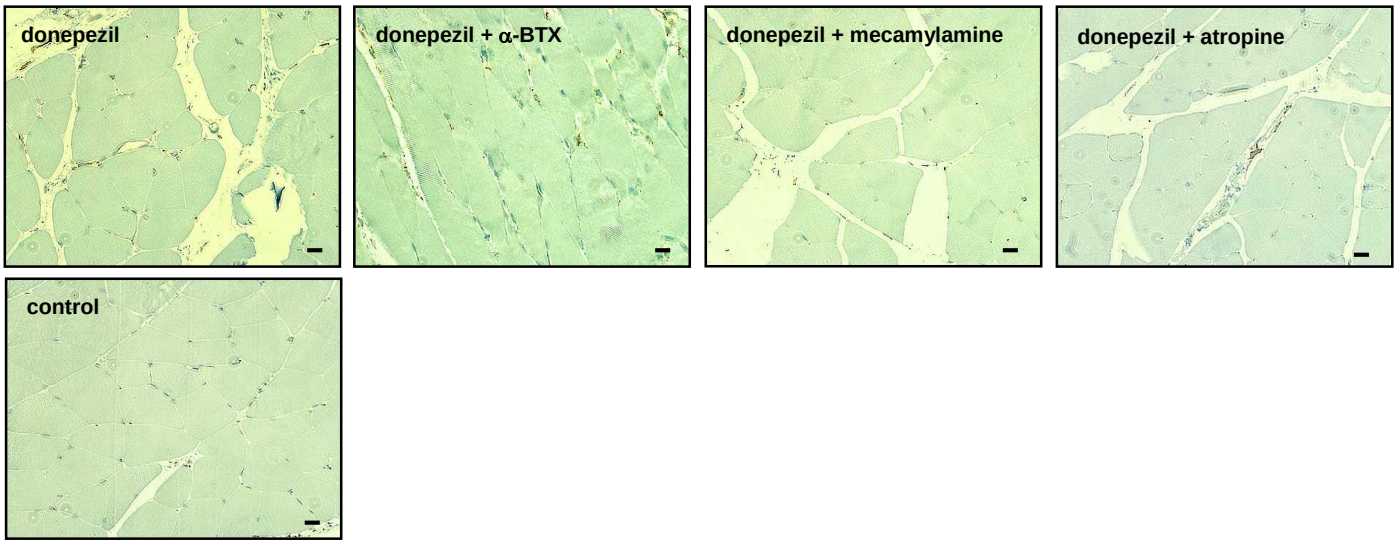

Kakinuma Y. et al.
Figure 2

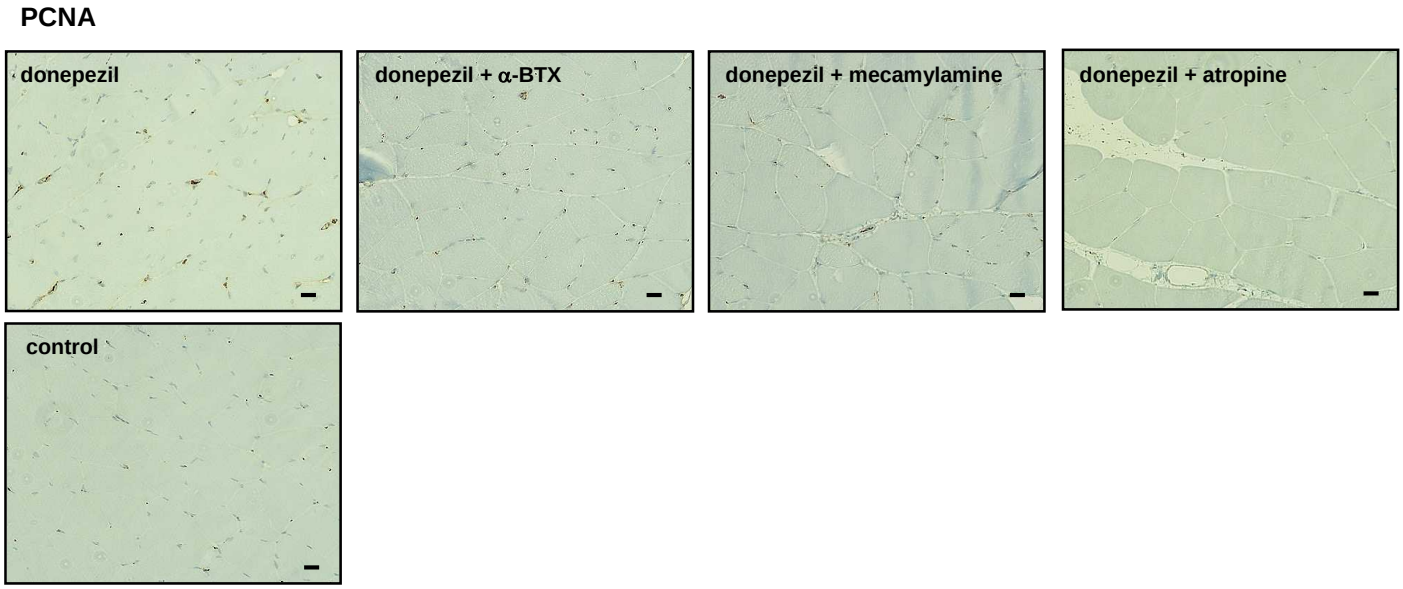

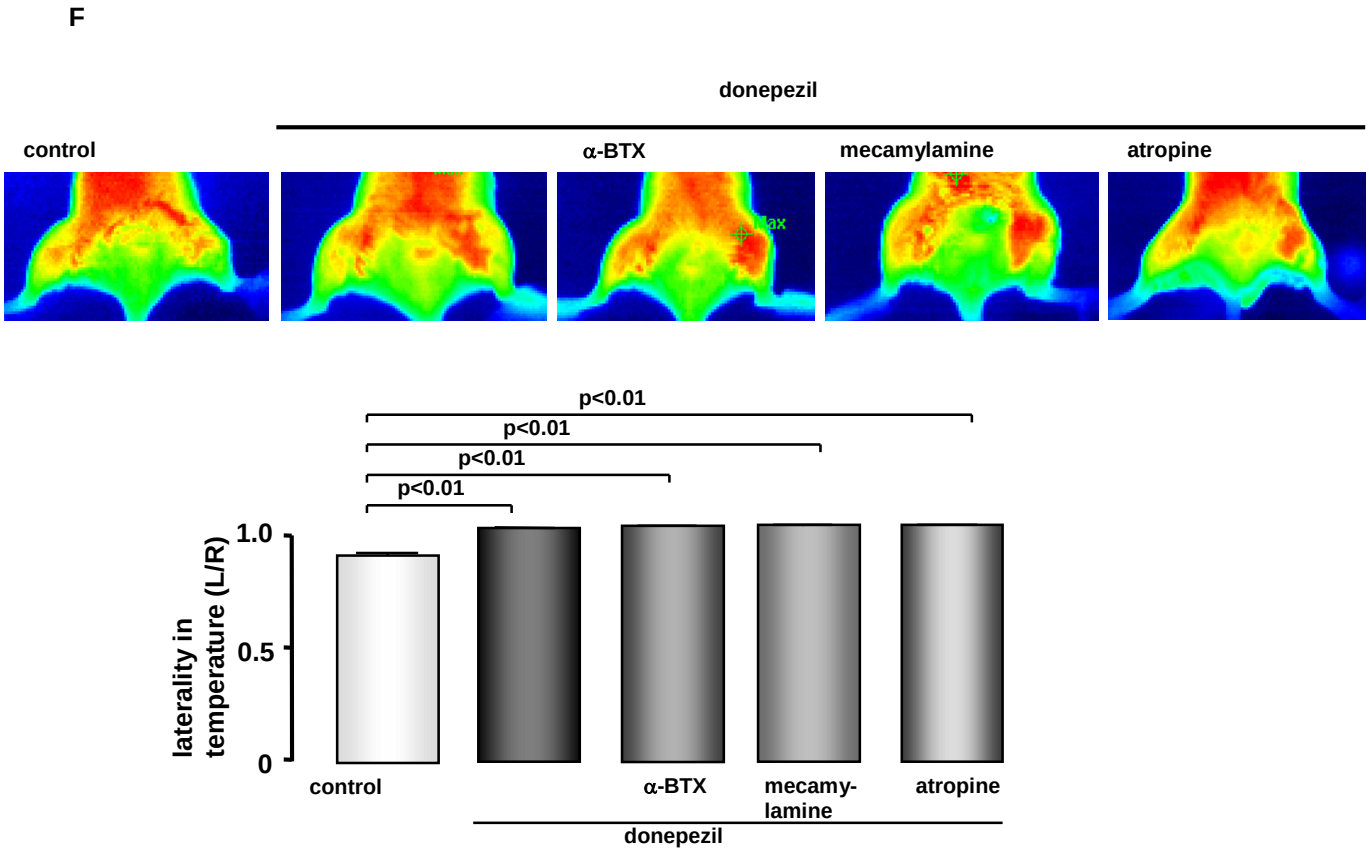

Kakinuma Y.
Figure 2

G

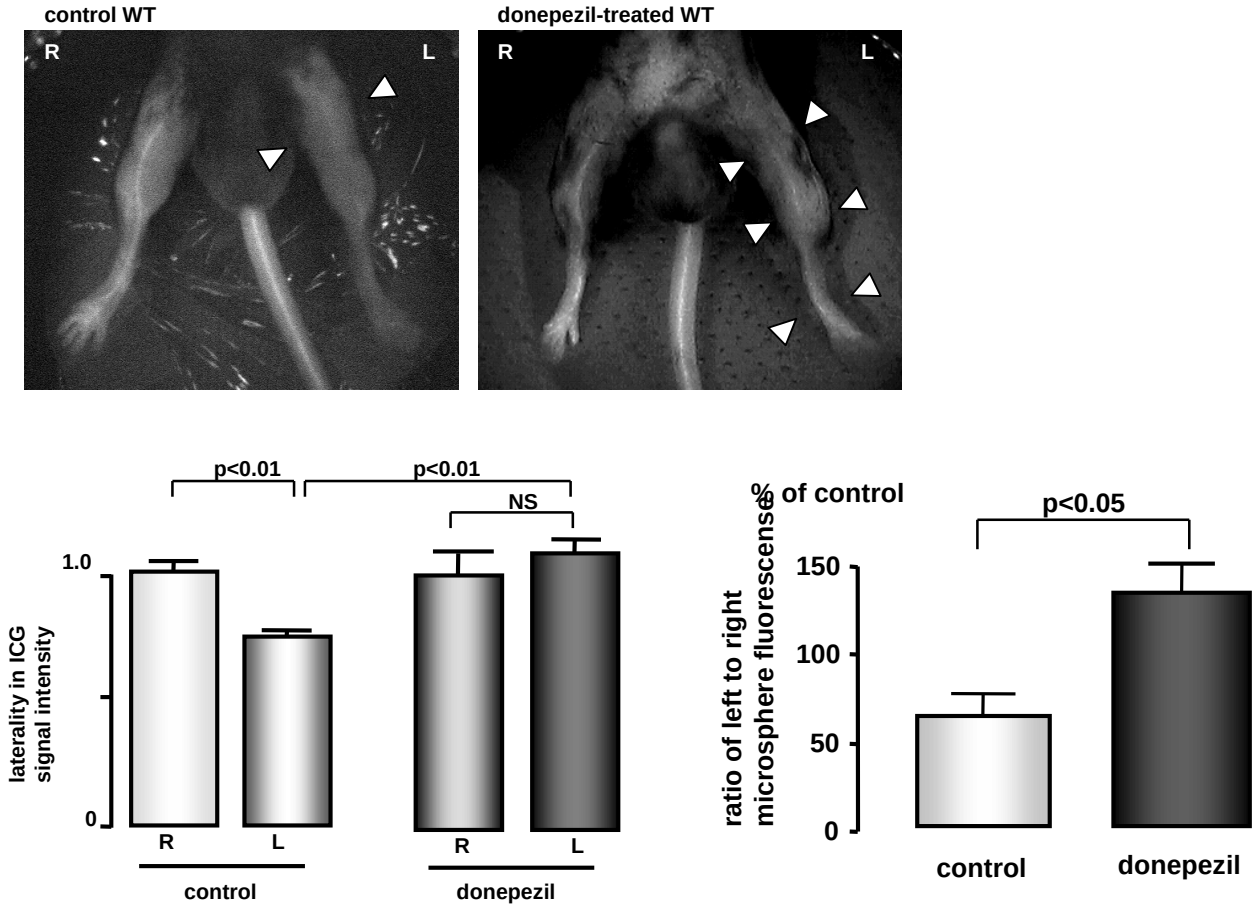

Figure 3

A

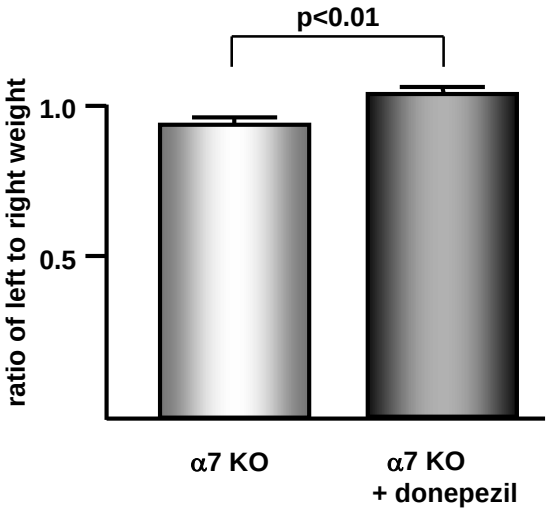

Kakinuma Y.
Figure 3

B

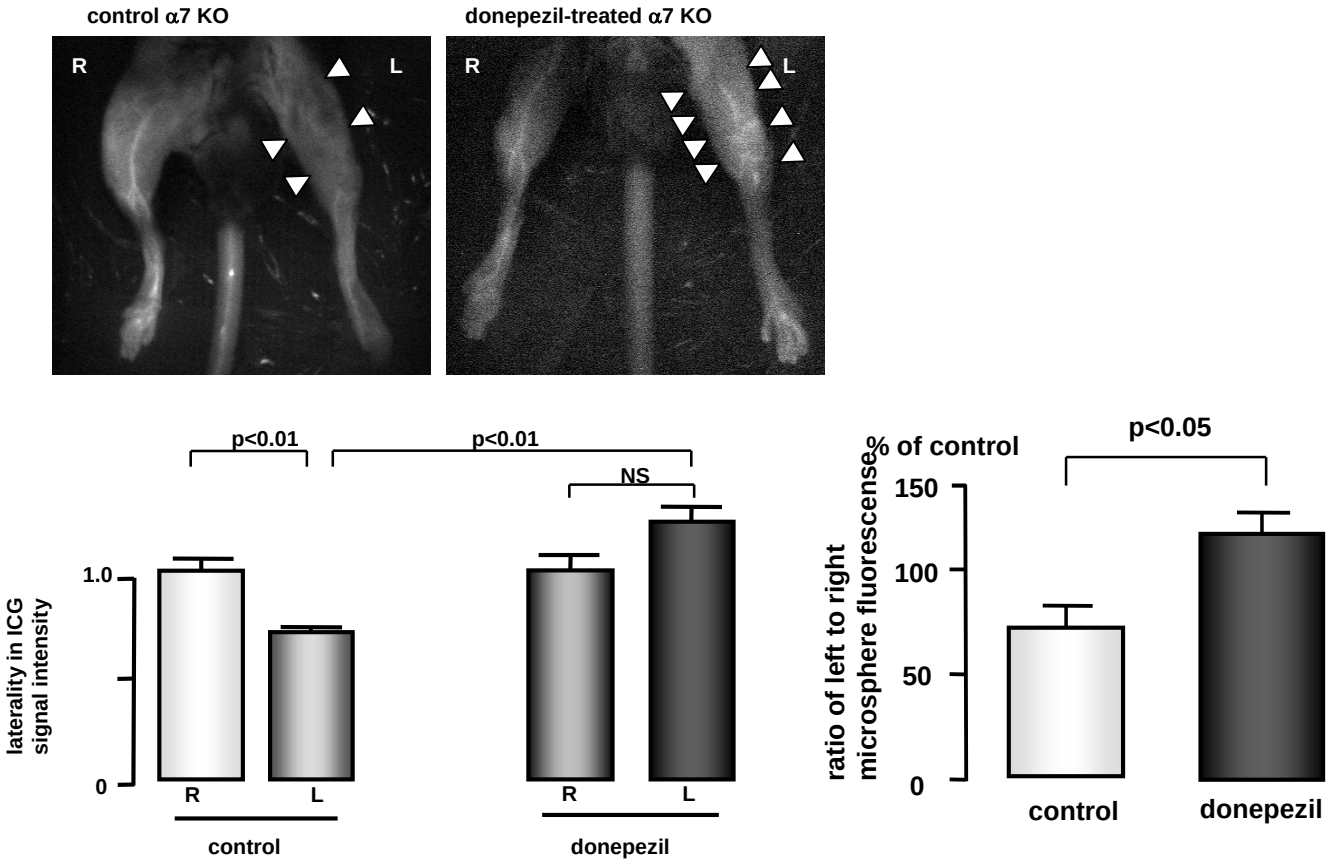

C

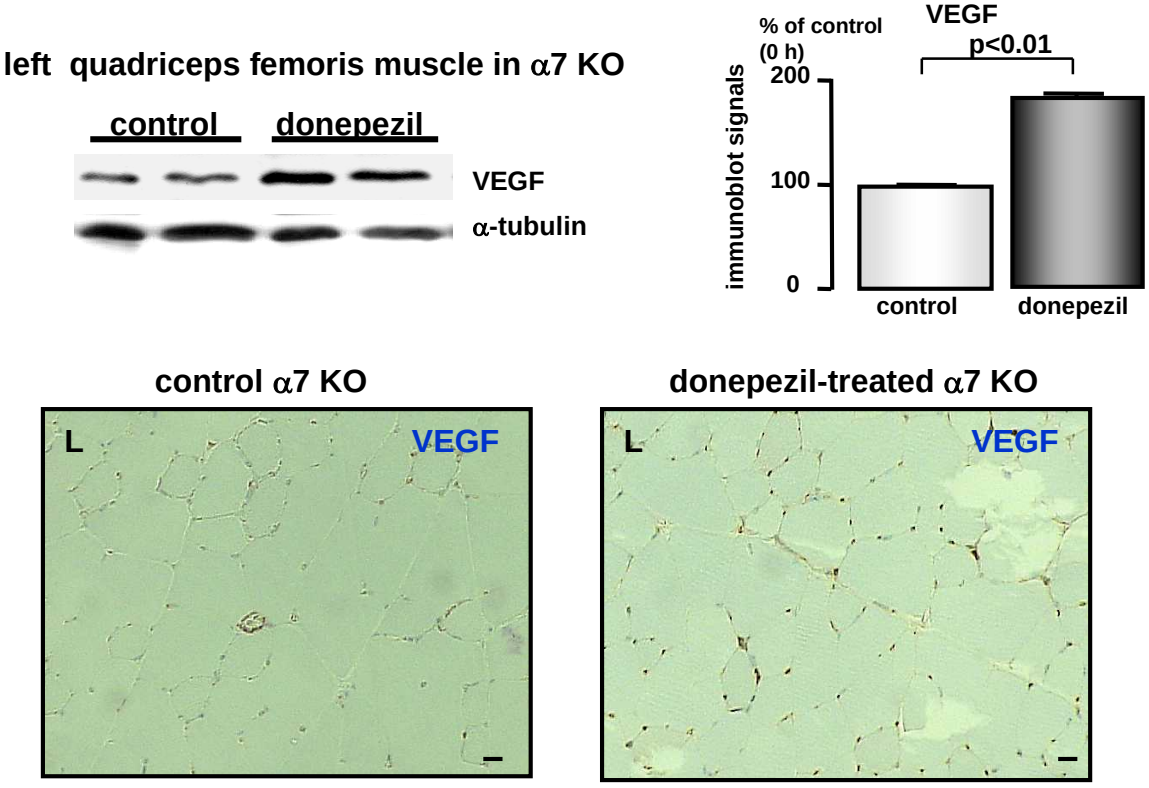

Kakinuma Y. et al.
Figure 3

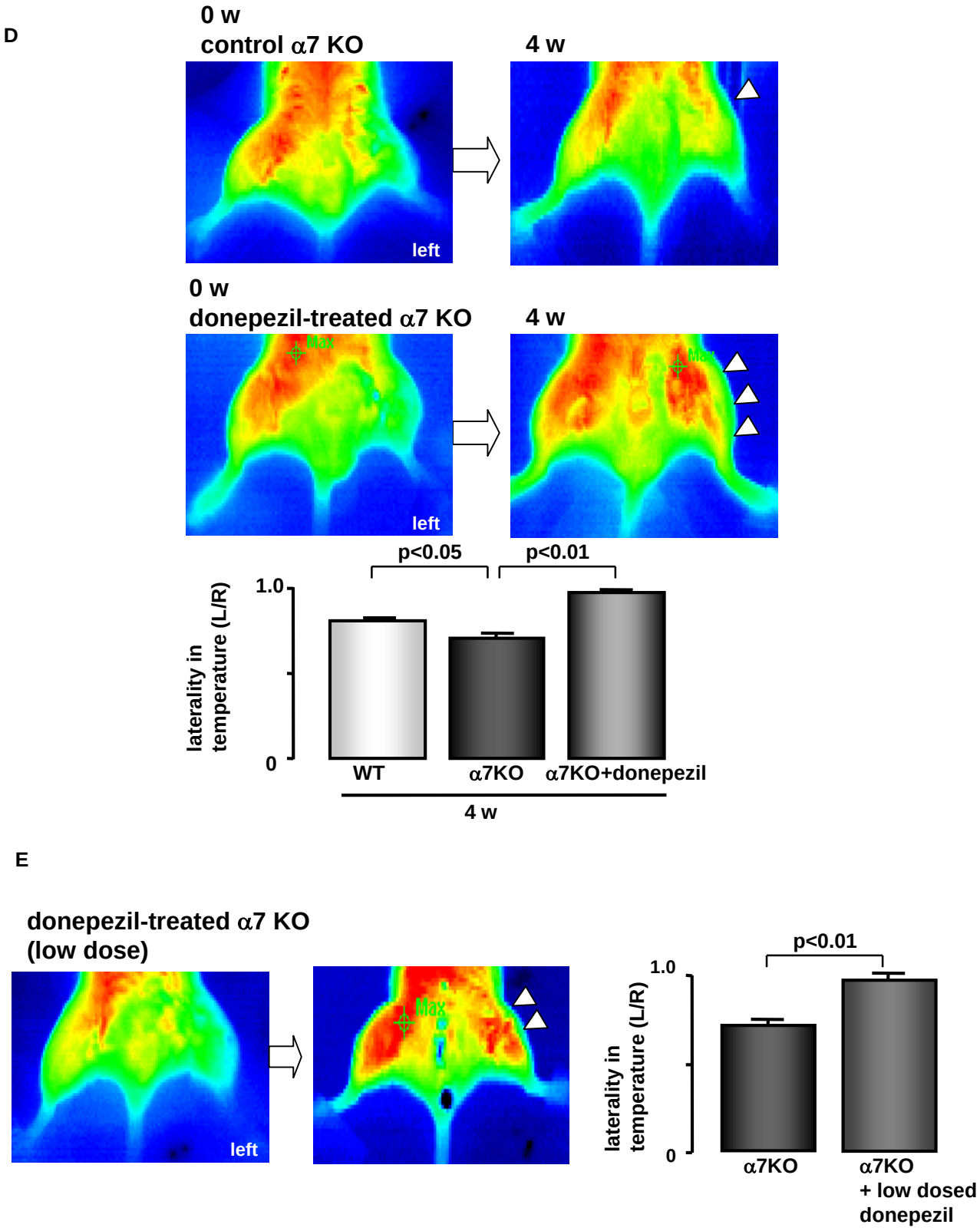

Kakinuma Y. et al.
Figure 4

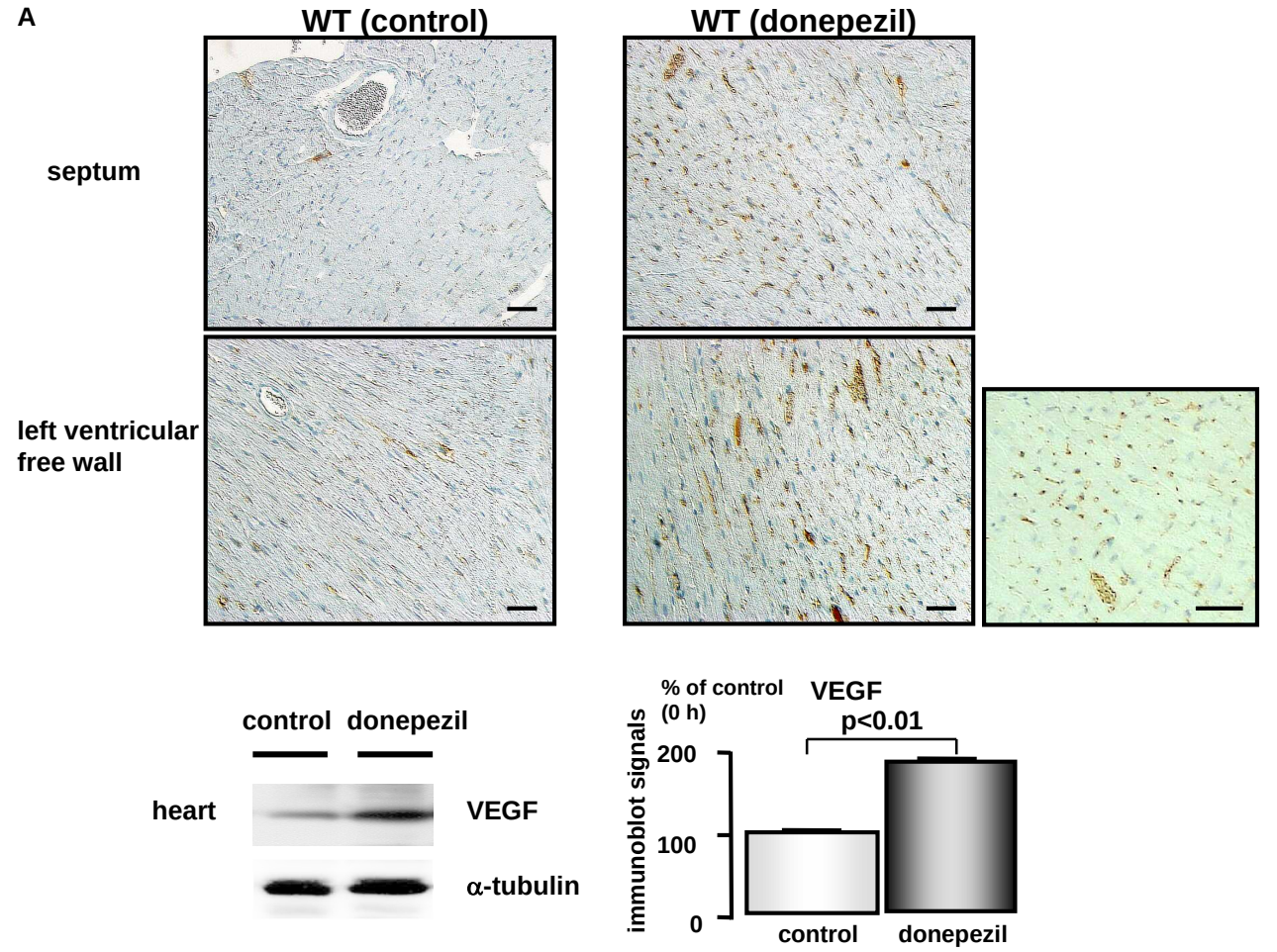

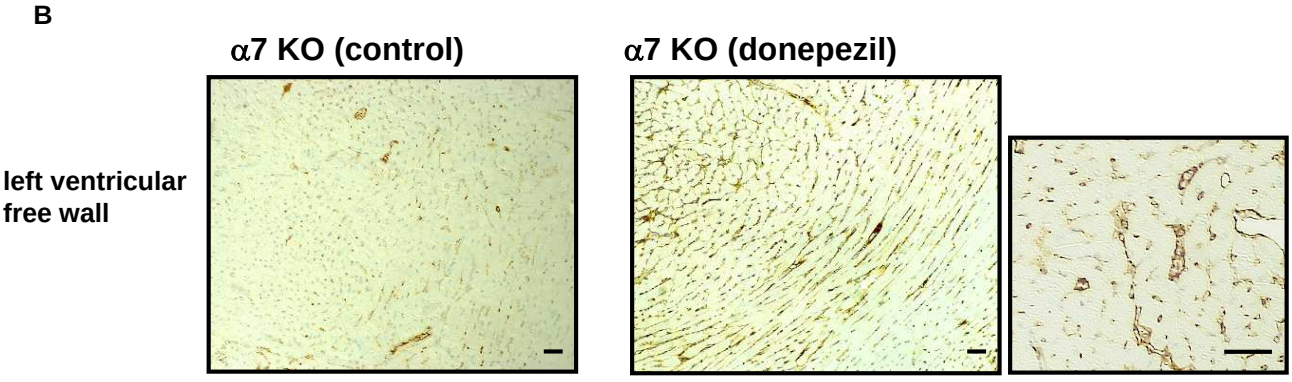

Kakinuma Y. et al.
Figure 4